

2011 International Nuclear Atlantic Conference - INAC 2011  
Belo Horizonte, MG, Brazil, October 24-28, 2011  
ASSOCIAÇÃO BRASILEIRA DE ENERGIA NUCLEAR - ABEN  
ISBN: 978-85-99141-04-5

# NON-DESTRUCTIVE ASSAY EMPLOYING 2D AND 3D DIGITAL RADIOGRAPHIC IMAGING ACQUIRED WITH THERMAL NEUTRONS AND REACTOR-PRODUCED RADIOISOTOPES

Maria Ines Silvani<sup>1</sup>, Gevaldo Lisboa de Almeida<sup>1</sup> and Ricardo T. Lopes<sup>2</sup>

<sup>1</sup> Instituto de Engenharia Nuclear (IEN/CNEN)  
Caixa Postal 68550, CEP 21945-970,  
Rio de Janeiro, RJ  
[msouza@ien.gov.br](mailto:msouza@ien.gov.br)

<sup>2</sup> Laboratório de Instrumentação Nuclear (COPPE/UFRJ)  
Caixa Postal 68509, CEP 21945-970,  
Rio de Janeiro, RJ  
[ricardo@lin.ufrj.br](mailto:ricardo@lin.ufrj.br)

## ABSTRACT

The inner structure of some objects can only be visualized by using suitable techniques, when safety reasons or expensive costs preclude the application of invasive procedures. The kind of agent rendering an object partially transparent, unveiling thus its features, depends upon the object size and composition. As a rough rule of thumb, light materials are transparent to gamma and X-rays while the heavy ones are transparent to neutrons. When, after traversing an object, they hit a proper 2-D detector, a radiograph is produced representing a convoluted cross section, called projection, of that object. Taking a large number of such projections for different object attitudes, it is possible to obtain a 3-D tomography of the object as a map of attenuation coefficients. This procedure however, besides a time-consuming task, requires specially tailored equipment and software, not always available or affordable. Yet, in some circumstances it is feasible to replace the 3-D tomography by a stereoscopy, allowing one to visualize the spatial configuration of the object under analysis. In this work, 2-D and 3-D radiographic images have been acquired using thermal neutrons and reactor-produced radioisotopes and proper imaging plates as detectors. The stereographic vision has been achieved by taking two radiographs of the same object at different angles, from the detector point of view. After a treatment to render them red-white and green-white they were properly merged to yield a single image capable to be watched with red-green glasses. All the image treatment and rendering has been performed with the software *ImageJ*.

## 1. INTRODUCTION

Non-destructive assays employing neutrons, x-rays or gamma-rays are sometimes the only suitable approaches to visualize the inner structure of objects which due to safety reasons or high costs should not be submitted to invasive procedures. Some of these approaches explore the partial transparency of the object to the radiation used as interrogation agent, by making the object to cast a *shadow* on a sensitive surface, such as a radiographic film, an imaging plate or some type of surface detector.

In any case, the shadow would represent an attenuation factor map for the specific attitude of the object with regard to the incoming radiation. Since each point in this map receives an amount of radiation which decreases exponentially with the product thickness times the

attenuation coefficient for the specific traversed material, a convolution occurs hiding thus the individual features of the object. The information, nevertheless, is not completely lost and can be at least partially retrieved by a proper unfolding technique if several maps are taken at different object orientations. This tomographic approach, however, requires the use of special pieces of equipment and software not always affordable or available. Yet, in some circumstances, it is feasible to replace a 3-D tomography by a stereo-radiographic image capable to exhibit the spatial inner structure of the inspected object.

Early in the eighties, x-ray stereo radiography has been applied for studies of damage in composites [1, 2], where the images were observed through an optical stereoscopic apparatus. More recently this technique has been recently extended [3] for neutron radiography employing the *red-green approach* where the black and white original images were colored and afterwards merged into a single image to be watched through red-green glasses in a monitor or as printed picture.

As different materials exhibit different attenuation properties for neutrons, x-rays and gamma-rays, the choice of the proper radiation depends upon the constitution and size of the object, provided that a suitable detector is available. The source of radiation, whatever its type, should possess some basic features in order to prevent penumbræ in the acquired images. Hence, point sources should be kept as small as possible, while extended sources should exhibit a low divergence, i.e., a narrow rocking curve.

In this work, 2-D and 3-D radiographic images have been acquired by transmission of thermal neutrons and 412 keV gamma-rays emitted by the reactor-produced isotope  $^{198}\text{Au}$ . Neutron and gamma-sensitive imaging plates have been employed as detector and temporary storage devices. The 3-D radiographic images have been obtained by the stereographic approach, where two images taken at different object attitudes were merged after being transformed into red-white and green-white colors. The resulting final image can then be observed through red-green glasses.

## 2. MATERIALS AND METHODS

All radiographic images have been acquired by transmission of thermal neutrons or by transmission of 412 keV gamma-rays emitted by  $^{198}\text{Au}$ . For both cases specific imaging plates have been used as detector and temporary storage device until their *development* by scanning with a  $0.5\mu\text{m}$ -diameter laser beam in the model BAS 2500 image reader from FUJI, yielding digital images.

### 2.1. Acquisition of Radiographic Images with Thermal Neutrons

The neutron radiographic images have been acquired with a beam of thermal neutrons available at the main port of the Argonauta research reactor at the *Instituto de Engenharia Nuclear* in Rio de Janeiro. A neutron-sensitive imaging plate, henceforth named NIP in this work, has been employed as detector which after exposure has been *developed* by the above mentioned imaging plate reader. All neutron radiographs have been acquired with a neutron flux of  $2.2 \times 10^5 \text{ n.cm}^{-2}.\text{s}^{-1}$  and an exposure time of 6 min.

Although the finest possible spatial resolution would be limited by the diameter of the laser beam used to scan the electrical image stored in the imaging plate, such a resolution can not be achieved, for other parameters contribute to degrade the final image. One of the most important of them is the divergence of the neutron beam [4], due to the unavoidable penumbra caused by neutrons coming from different directions. This divergence expressed by the FWHM of the related rocking curve of reaches  $1^{\circ} 16'$  [5].

In order to establish a correlation between the spatial resolution and the object-detector gap, a special test-object containing cadmium inserts attached to an aluminum sheet was placed between the reactor main port and the NIP as shown in Fig. 1. As seen in this figure, farther inserts yield blurrier images, defining thus poorer spatial resolutions.

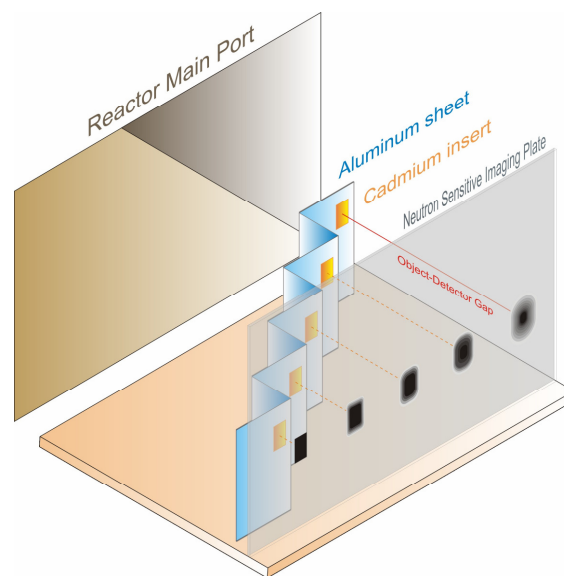


**Figure 1. Arrangement used to determine the curve Spatial Resolution x Object-Detector gap.**

The first step to determine these resolutions is to obtain the Line Spread Function - LSF, for each spot, through differentiation of the Edge Response Function - ERF. This function is obtained by plotting the optical density in the neighborhood of the spot edges along a perpendicular direction. A discrete Fourier transform is then applied to each LSF yielding the Modulation Transfer Function - MTF.

A family of these curves for several object-detector gaps ranging from 3.5 to 53.5 mm is shown in Fig. 2. These curves incorporate obviously not only the penumbræ contribution to the image degradation but also the neutron scattering.

It is generally agreed [6] that an image has an acceptable quality when the modulation, i.e., the ratio of amplitude to the mean value reaches at least 0.1. Hence, a cut-off of the modulation at this level furnishes the maximal spatial frequency capable to fulfill this

requirement Its inverse furnish the spatial resolution as function of the object-detector clearance, as shown in Fig. 3.

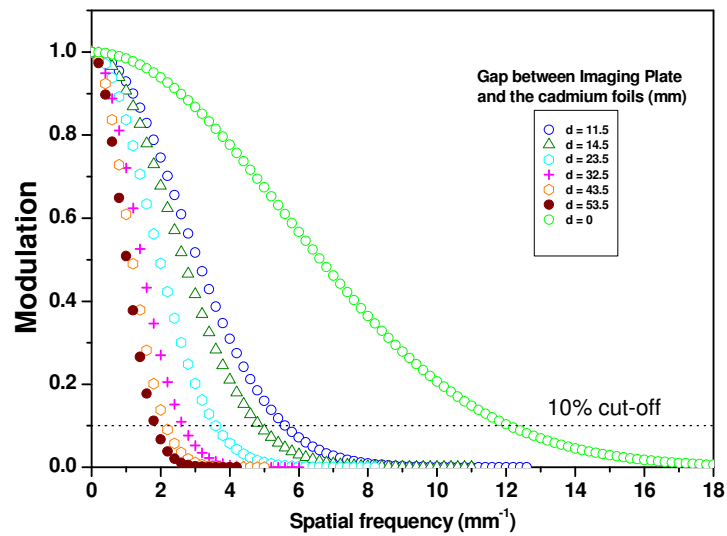


**Figure 2.** Family of MTF curves for several object-detector gaps. The cut-off at a modulation of 10% furnishes the maximal spatial frequency still capable to produce images of acceptable quality.

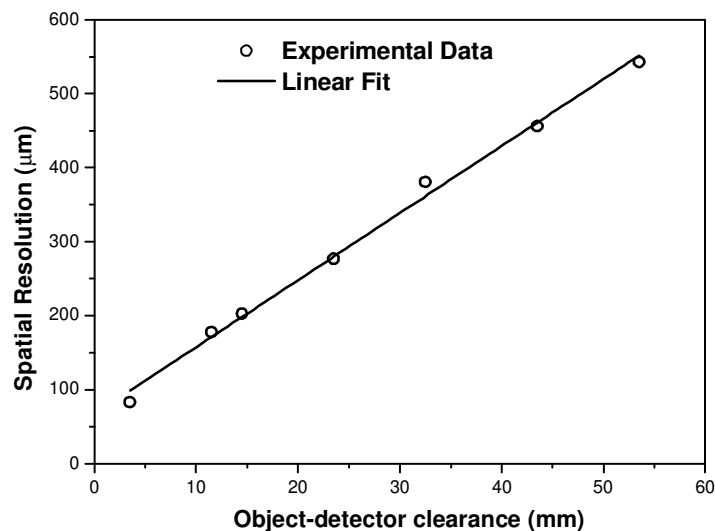


**Figure 3.** Spatial resolution of the neutron radiographic system against the object-detector gap. The intrinsic spatial resolution for a *zero* gap is about 60  $\mu\text{m}$ .

As seen in Fig.3, the spatial resolution is degraded fairly linearly with the object-detector gap. With this curve, it is possible to make an estimative about the radiograph quality of an object which, due to its thickness, has portions differently apart from the imaging plate.

## 2.2. Acquisition of Radiographic Images with 412 keV Gamma-Rays from $^{198}\text{Au}$

These radiographic images have been obtained using a system comprised by a  $^{198}\text{Au}$  source produced in the Argonauta reactor. It was placed 30 cm apart from a 20 x 40 cm X-ray-sensitive imaging plate, henceforth called XIP in this paper, enclosed within an aluminum chassis to protect it from the environmental light. The source *appearance* - as seen by the detector - has been kept as punctual as possible by limiting the mass of the original gold sample, reducing hence the penumbra effects.

Due to the low neutron flux available, both, irradiation and exposure times have to be lengthened. Yet, as the exposure phase is cheaper and can occur unattended, the irradiation time has been limited to some hours, while the exposure required a couple of days in order to reach an image with adequate contrast. Typical irradiation times were 3 hours under a neutron flux of  $3 \times 10^9 \text{ n.cm}^{-2}.\text{s}^{-1}$ . After exposure, the imaging plate was read by the model BAS-2500 Scan from *Fujifilm* provided with a  $50 \mu\text{m}$ -diameter laser beam. Further details can be found elsewhere [7].

## 2.3. Methodology employed to produce the Stereo-radiographic Images

A stereoscopic image is produced in the brain because an object is observed under different angles by the eyes. Therefore to achieve this effect two radiographs should be taken as if they were seen by the eyes. So, after the first exposure, the object is rotated by an angle of  $10^\circ$ , and the XIP replaced by another one dully *cleaned* which is exposed furnishing the second radiograph. The larger the angle, the closer an image appears to the observer, but too large angles create convergence problems making the fusion of the images in the brain difficult.

After acquisition the two digital black & white images are transformed into red & white and green & white ones which are afterwards merged to yield a single image which can be observed in a PC monitor or in a printed paper with red & green eyeglasses. The observer perceives then a black & white stereoscopic image. All the process has been carried out with the *ImageJ*, but it can be performed using the *Adobe Photoshop* software as well.

## 3. RESULTS

Neutron and gamma radiographic images of several components and pieces of equipment have been acquired, some of them taken at two different spatial orientations with regard to the set source-detector in order to compose stereographic images. Due to the different attenuation coefficients of thermal neutrons and gamma-rays for different materials the images produced by these agents exhibit complementary information. It is thus illustrative to depict these images together for the sake of comparison.

### 3.1. Radiographic Images acquired with Thermal Neutrons and 412 keV Gamma-Rays

In this section, 2-D radiographic images of a hard disk driver, a stepper motor, and an aircraft altimeter, taken with 412 keV gamma-rays are shown as follows.

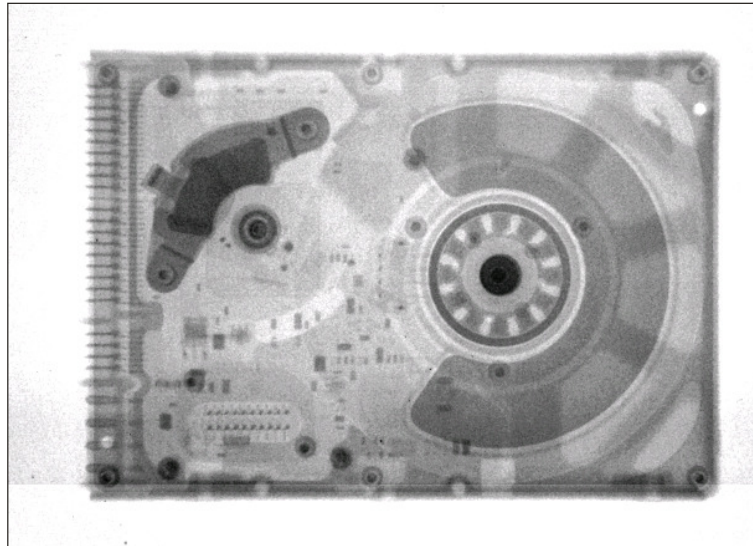


**Figure 4. Gamma radiograph of a hard disk driver acquired with a reactor-produced  $^{198}\text{Au}$  source.**

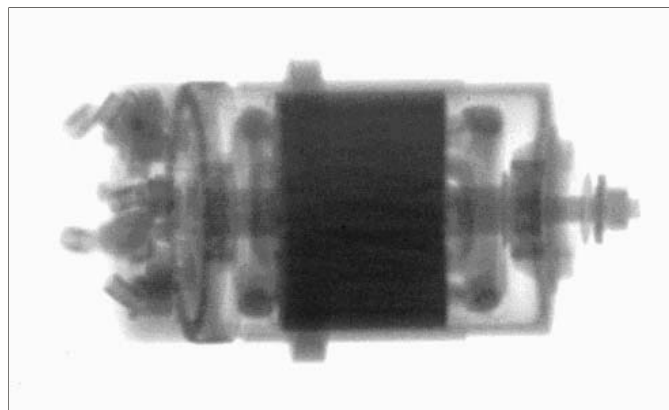


**Figure 5. Gamma radiograph of a stepper motor acquired with a reactor-produced  $^{198}\text{Au}$  source.**

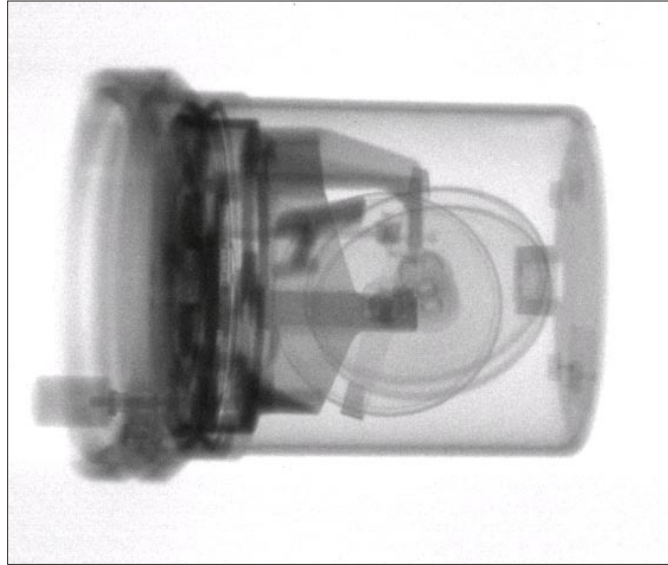


**Figure 6. Gamma radiograph of an aircraft altimeter acquired with a reactor-produced  $^{198}\text{Au}$  source.**

Additionally neutron and gamma-ray radiographs of a stator blade, - a component of an aircraft turbine used to straighten the air flow, improving thus the thrust - are shown in Fig. 7.

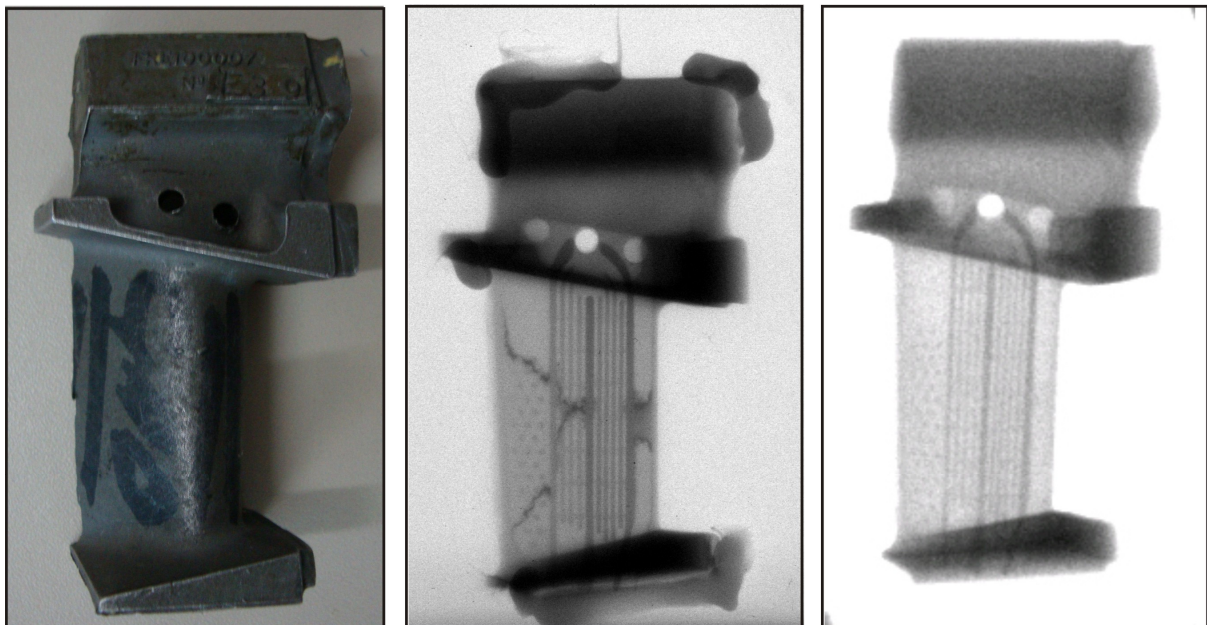


**Figure 7. Photography (left) Neutron (centre) and gamma-ray (right) radiographs of a turbine stator blade employed to straighten the air flow.**

A comparison between the two radiographic images shows, in both of them, darker vertical strips corresponding to the inner walls of the air cooling channels. This cooling is a must considering the high temperatures occurring during the turbine operation. Moreover, the neutron radiograph exhibits additional features in the cooling channel region as irregular darker strips for instance. These irregularities are caused by the presence of the remaining ceramic material which has been not completely removed after the manufacturing process. It was made visible by impregnation with a gadolinium solution, during the quality control. The stuff seen around the piece is a glue employed to fix the device on the NIP during the exposure.

### 3.1. Stereo-radiographic Images acquired with Neutrons and 412 keV Gamma-Rays

Stereo-radiographic images of an old-fashioned film camera taken with neutrons and gamma rays are shown in Fig.8. These images should be watched through red-green glasses (red lens on left). At first sight one realizes that the image acquired with gamma-rays exhibits a better resolution. This happens due to the divergence of the neutron beam which casts penumbrae on the NIP. Yet, in spite of its poorer quality this image still furnishes valuable information regarding the inner structure of the object under inspection. It can be noticed, for instance, among many other observable features, that the film take-up spool, at the right side, appears broader in the neutron-acquired image. This is due to the neutron-attenuating plastic hull enclosing the metallic axis of the spool, which is clearly seen in the gamma-acquired image.

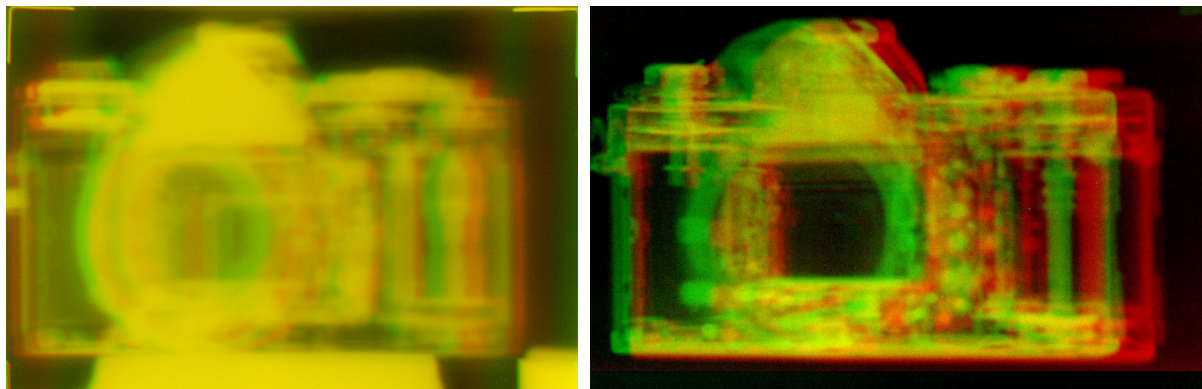


**Figure 8. Neutron (left) and gamma-ray (right) stereo-radiographs of an old-fashioned film camera. The divergence of the neutron beam degrades substantially the image quality.**

## 4. CONCLUSIONS

Radiographic images obtained by transmission of thermal neutrons and of 412 keV gamma-ray emitted by the reactor-produced  $^{198}\text{Au}$  have been used as a tools for non-destructive assay of several pieces of equipment, devices and components. Imaging plates designed to operate with thermal neutrons and with x-rays have been employed as detector. The spatial resolution



for neutron acquired images as function of the object-detector gap has been deduced from the Modulation Transfer Functions experimentally measured.

In spite of the high photon energy used, surpassing the x-ray range for which the imaging plates have been designed, radiographic images of good quality have been obtained. The inner spatial structure of the inspected objects has been as well visualized by stereoscopy employing radiographs taken at different object attitudes, which after a coloring process were merged in a single one and watched through red-green glasses. In spite of its intrinsic limitations, this simple technique provides valuable information about the object otherwise only available through a more refined and expensive 3D tomography.

The utilization of a reactor-produced radioisotope as source for gamma-ray radiography has shown to be a suitable option for research centers where a reactor is available, as it make possible to choose gamma-ray emitters best suited to the aimed application. Due to the low neutron flux available and the limitation on the mass of the sample, tens of exposure hours were required to achieve an image with adequate contrast. Yet, it does not constitute a serious hindrance, as the exposure process can be carried out without any human intervention or surveillance.

## REFERENCES

1. Rummel, W. D., Tedrow, T. and Bunkerhoff, H. D., "Enhanced Stereoscopic NDE of Composite Materials," **AFWAL Technical Report**, 80-3053 (1980).
2. Sendekyj, G. P., Maddux, G. E. and Porter, E., "Damage Documentation in Composites by Stereo Radiography, in *Damage in Composite Materials*, **STP 775**, K. L. Reifsnider, Editor, American Society for Testing and Materials, pp. 16-26 (1982).
3. Silvani, M. I., Almeida, G. L. Rogers, J. D., Lopes R. T., "Stereoscopic Radiographic Images with Thermal Neutrons", *Nuclear Instruments and Methods in Physics Research A*, <http://dx.doi.org/10.1016/j.nima.2010.09.051>
4. Almeida, G. L. Silvani, M. I., Furieri, R. A., Gonçalves M. J., Lopes R. T., "Forecasting the effect of neutron beam divergence on the quality of tomographic images". *Nuclear Instruments and Method in Physics Research A*, **579**, Issue 1, pp. 231-234 (2007).
5. Almeida, G. L., Silvani, M. I., Lopes R.T., "Evaluation of the Divergence of a Thermal Neutron Beam using a Position Sensitive Detector", *Brazilian Journal of Physics*, **35**, 3B, pp.771-774 (2005).
6. ASTM E 1441-95 and 1570-95a, "Non-Destructive Testing Radiation Methods. Computed Tomography. Guide for Imaging and Practice for Examination", **ISO/TC 5 N118** (1996).
7. Silvani, M. I., Almeida, G. L., Furieri, R., Lopes R.T., "On the Performance of X-ray Image Plates in Gamma Radiography employing Reactor-Produced Radioisotopes", *XXXIII Brazilian Workshop on Nuclear Physics AIP Conference Proceedings 1351*, <http://proceedings.aip.org/> (2011).